Munc13 controls the location and efficiency of dense-core vesicle release in neurons

Rhea van de Bospoort,[1] Margherita Farina,[1] Sabine K. Schmitz,[1] Arthur de Jong,[1] Heidi de Wit,[1] Matthijs Verhage,[1,2] and Ruud F. Toonen[1]

[1]Department of Functional Genomics, Center for Neurogenomics and Cognitive Research, Neuroscience Campus Amsterdam; [2]Department of Clinical Genetics, VU University Medical Center; VU University, 1081 HV Amsterdam, Netherlands

Neuronal dense-core vesicles (DCVs) contain diverse cargo crucial for brain development and function, but the mechanisms that control their release are largely unknown. We quantified activity-dependent DCV release in hippocampal neurons at single vesicle resolution. DCVs fused preferentially at synaptic terminals. DCVs also fused at extrasynaptic sites but only after prolonged stimulation. In *munc13-1/2*–null mutant neurons, synaptic DCV release was reduced but not abolished, and synaptic preference was lost. The remaining fusion required prolonged stimulation, similar to extrasynaptic fusion in wild-type neurons. Conversely, Munc13-1 overexpression (M13OE) promoted extrasynaptic DCV release, also without prolonged stimulation. Thus, Munc13-1/2 facilitate DCV fusion but, unlike for synaptic vesicles, are not essential for DCV release, and M13OE is sufficient to produce efficient DCV release extrasynaptically.

Introduction

Neuronal dense-core vesicles (DCVs) contain neuropeptides, neurotrophic factors, monoamines, and other modulatory substances that are essential during brain development and regulate synaptic plasticity in the adult brain (McAllister et al., 1999; Huang and Reichardt, 2001; Poo, 2001; Samson and Medcalf, 2006). To date, >50 biologically active peptides have been identified that have profound effects on brain and body function. Not surprisingly, dysregulation of DCV signaling is associated with many diseases, such as mood and cognitive disorders, obesity, and diabetes (Meyer-Lindenberg et al., 2011). DCVs are filled with cargo at the Golgi network (Kim et al., 2006) and transported through axons and dendrites via microtubule-based motors of the kinesin and dynein families (Hirokawa et al., 2009; Schlager and Hoogenraad, 2009). Calcium influx triggers DCV release from synaptic and extrasynaptic regions on axons and dendrites (Hartmann et al., 2001; Ludwig and Leng, 2006; de Wit et al., 2009b; Matsuda et al., 2009; Knobloch et al., 2012), and previous work identified several stimulation paradigms that trigger DCV fusion (Bartfai et al., 1988; Verhage et al., 1991; Hartmann et al., 2001; Matsuda et al., 2009). Yet, little is known about the molecules that control the location and kinetics of DCV secretion in mammalian neurons.

In contrast to the relative lack of understanding of DCV fusion, synaptic vesicle (SV) fusion mechanisms are much better understood (Jahn and Scheller, 2006; Südhof and Rothman, 2009). SVs cluster at active zones, fuse upon calcium influx, and locally recycle at the presynaptic terminal (Südhof, 2004). DCVs are generally more dynamic (de Wit et al., 2006; Shakiryanova et al., 2006; Matsuda et al., 2009) and are present in synaptic terminals as well as neurites and perikarya, but it is not clear whether DCVs specifically cluster at synaptic terminals or use activity-dependent recruitment mechanisms as seen in *Drosophila melanogaster* neuromuscular junctions (Shakiryanova et al., 2006; Wong et al., 2012). Hence, transport and release characteristics of SVs and DCVs differ to some extent, but they also share properties such as the requirement for functional SNARE complexes and calcium influx to initiate fusion (Xu and Xu, 2008). Therefore, proteins that function in SV release (Garner et al., 2000; Rosenmund et al., 2003; Verhage and Toonen, 2007; de Wit et al., 2009a; Sørensen, 2009) may have similar functions in DCV release in neurons. Yet, no candidates have been investigated to date.

Correspondence to Matthijs Verhage: matthijs.verhage@cncr.vu.nl; or Ruud F. Toonen: ruud.toonen@cncr.vu.nl

Abbreviations used in this paper: AP, action potential; a.u., arbitrary unit; DCV, dense-core vesicle; DIV, day in vitro; KO, knockout; M13DKO, Munc13-1/2 double KO; M13OE, Munc13-1 overexpression; NPY, Neuropeptide Y; SpH, superecliptic pHluorin; SV, synaptic vesicle; WT, wild type.

The Rockefeller University Press $30.00
J. Cell Biol. Vol. 199 No. 6 883–891
www.jcb.org/cgi/doi/10.1083/jcb.201208024

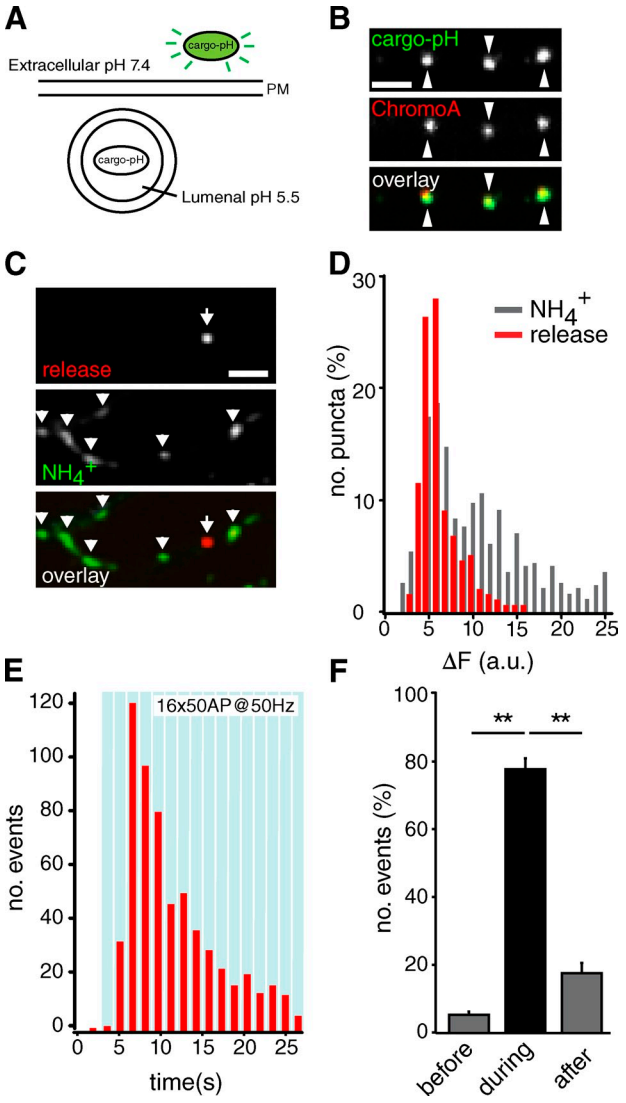

Figure 1. **Optical sensor for DCV release in neurons.** (A) Schematic representation of an optical reporter for DCV release that allows visualization of single DCV fusion events. PM, plasma membrane. (B) Confocal image of a neuron transfected with Semaphorin-3a–pHluorin (cargo-pH) and stained for endogenous DCV cargo chromogranin A (ChromoA) showing complete overlap (arrowheads). (C) Image series showing a cargo-pHluorin release event (arrows) and the NH_4^+ response to reveal all vesicles in the neurite (arrowheads). (D) Normalized frequency distribution of ΔF for DCV release events measured with Semaphorin-3a–pHluorin and ΔF upon NH_4^+ perfusion (NH_4^+: 395 puncta, 7 cells; release: 293 puncta, 30 cells; median ΔF release = 5.4 a.u.; median ΔF NH_4^+ = 6.0 a.u.). (E) Frequency distribution of DCV release events measured with Semaphorin-3a–pHluorin (570 release events in 53 cells; blue bars, 16 bursts of 50 APs at 50 Hz). (F) DCV release events during 60 s before stimulation, during stimulation, and during 70 s after stimulation (before: 1 ± 0.6; during: 16 ± 3.4; after: 5 ± 1.3 vesicles/cell; n = 21 cells, n = 3). **, $P < 0.01$. Data are plotted as means with SEM. Bars, 2 µm.

To assess the spatial and temporal characteristics of neuronal DCV release in a quantitative way, we used an optical probe to visualize single DCV release events in hippocampal neurons. We found that DCVs are preferentially released from synaptic terminals. Release onset is faster, and the rate of release is higher at synapses compared with extrasynaptic sites. To unravel underlying molecular mechanisms, we investigated the role of the Munc13 family members Munc13-1 and -2, SV priming proteins that are essential for SV release (Augustin et al., 1999; Rhee et al., 2002; Varoqueaux et al., 2002; Basu et al., 2007). We show that deletion of Munc13-1/2 strongly decreased but did not abolish DCV release, whereas Munc13-1 overexpression (M13OE) resulted in increased DCV release. Strikingly, both the absence and overexpression of Munc13 changed the synaptic preference of DCV release: Munc13 deletion specifically reduced synaptic release events, whereas overexpression increased release only from extrasynaptic sites. Thus, in addition to its fusion-promoting role, Munc13 also affects the localization of DCV release, and Munc13 overexpression is sufficient to promote efficient DCV release at extrasynaptic sites along the plasma membrane.

Results and discussion

Optical sensor for DCV release in neurons

To study neuronal DCV release, we used reporters generated by fusing the canonical DCV cargo proteins Neuropeptide Y (NPY) or Semaphorin-3a to pH-sensitive EGFP (pHluorin; Fig. 1 A and Fig. S1). We have previously shown that these cargo, when overexpressed in mouse hippocampal neurons, are coexpressed in the majority of DCVs with an almost 90% overlap with endogenous DCV cargo Chromogranin A (de Wit et al., 2009b; Fig. 1 B). DCV-pHluorin release events become visible as bright diffraction limited spots (Fig. 1 C). To test whether these spots represent single or multiple DCV release events, the fluorescence intensity increase (ΔF) of individual release events was compared with the ΔF of DCV puncta upon NH_4^+ superfusion (to dequench intravesicular pHluorin; Fig. 1 D). The ΔF intensity plot upon NH_4^+ application showed a skewed distribution with a major population at ±6 arbitrary units (a.u.) that overlapped with the ΔF of individual release events, suggesting that the latter are generally single vesicle fusion events (Fig. 1 D).

To initiate release of DCVs, neurons were stimulated with 16 bursts of 50 action potentials (APs) at 50 Hz. This stimulus is optimal for release of the neuropeptide brain-derived neurotrophic factor from hippocampal neurons (Hartmann et al., 2001). DCV release was strongly coupled to this stimulation and resulting calcium influx (Fig. 1 E and Fig. S1). Only a few DCVs were released before or after the stimulus train (Fig. 1, E and F; and Fig. S1). Other stimulation paradigms were not as effective in releasing DCVs (Fig. S1).

DCVs do not accumulate at synapses, but DCV release is enriched and more efficient at these sites

Many proteins involved in SV fusion are enriched in synaptic terminals (Südhof, 2004). If these proteins were also involved in DCV release, DCV release should be enriched at synaptic sites. To test this, we quantified synaptic and extrasynaptic release (Fig. 2, A and B) using the SV protein synapsin to visualize synapses in living neurons (Gitler et al., 2004). Synapsin-mCherry fusion proteins formed discrete puncta along the dendrite that colocalized with endogenous VAMP2, confirming that synapsin-mCherry is correctly localized to synapses (our previous results [de Wit et al., 2006]; Fig. S1 F).

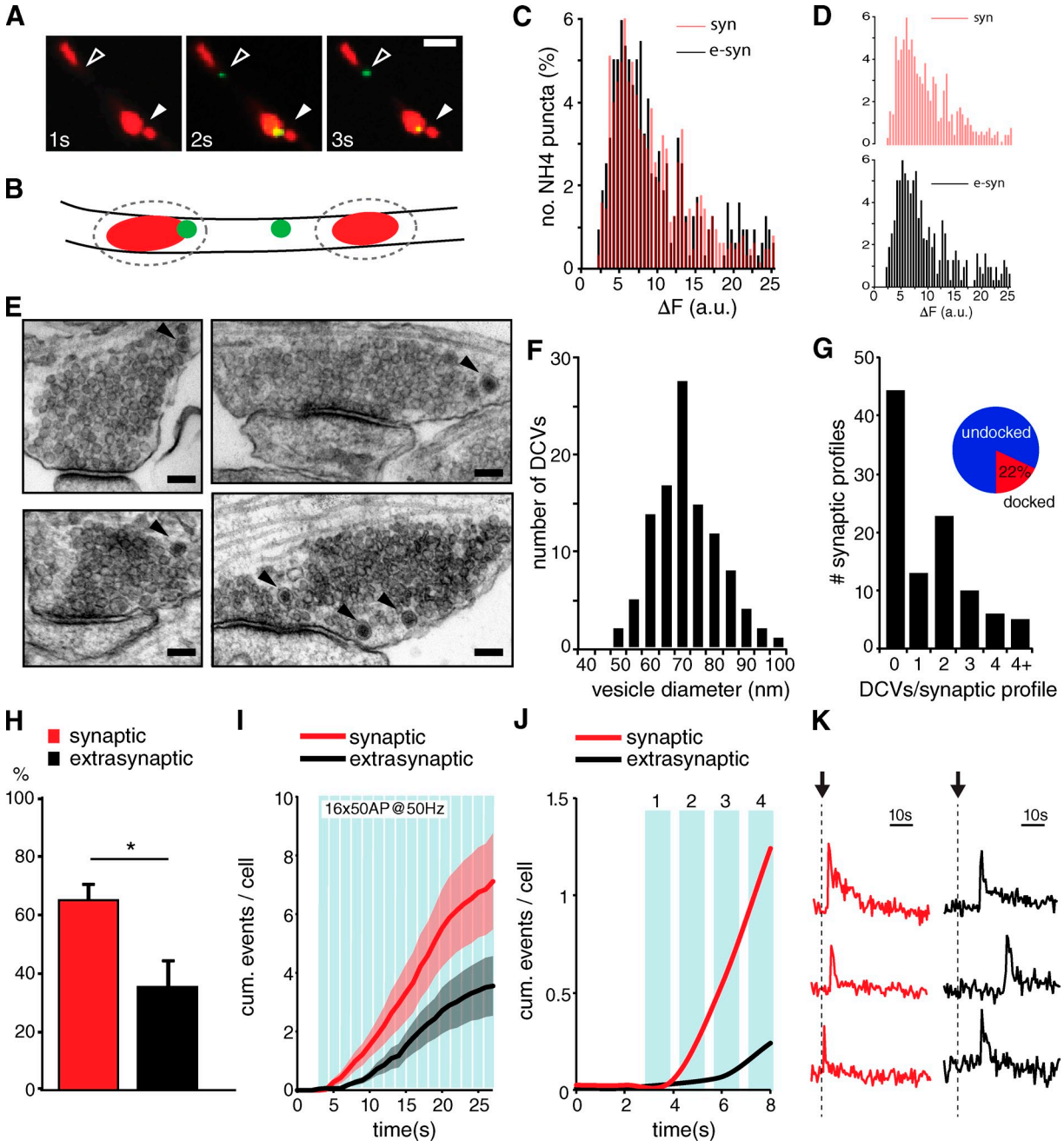

Figure 2. **DCV release is enriched and more efficient at synapses although DCVs do not accumulate at synaptic regions.** (A) Example of a synaptic (filled arrowheads) and an extrasynaptic release event (open arrowheads). Synapsin-mCherry is shown in red, and release events are shown in green. Bar, 1 µm. (B) Cartoon showing a synaptic (left green dot) and extrasynaptic (right green dot) release event. (C) Overlay of frequency distribution of ΔF upon NH_4^+ application for synaptic (syn) DCV puncta (synaptic 589 puncta) and extrasynaptic (e-syn) DCV puncta (extrasynaptic 612 puncta). (D) Individual frequency distributions of ΔF upon NH_4^+ application. (E) Electron micrographs of synaptic terminals that harbor DCVs. Arrowheads point to DCVs. Bars, 100 nm. (F) Diameter of DCVs in electron micrographs (mean diameter: 68.9 ± 1.0 nm, 146 DCVs in 7 cells). (G) Number of DCVs per synaptic profile (102 synapses in 7 cells). Inset, ±22% of synaptic DCVs is docked to the plasma membrane (undocked, 113; docked, 33; total, 146). (H) Percentage of synaptic and extrasynaptic DCV release events measured with Semaphorin-3a–pHluorin (235 synaptic release events, 131 extrasynaptic release events; n = 34 cells, n = 3; *, P < 0.05). (I) Cumulative number of release events per cell for synaptic and extrasynaptic events. (Synaptic release rate: 0.26 ± 0.03 vesicles/s; extrasynaptic: 0.13 ± 0.02 vesicles/s). Shading represents SEM. (J) Cumulative number of events during the first four bursts (blue bars 1, 2, 3, and 4 represent 50 APs at 50 Hz) for synaptic and extrasynaptic events. (K) Example traces of synaptic (red) and extrasynaptic (black) release events. Arrows mark start of the stimulation. Data are plotted as means with SEM.

We first tested whether DCVs accumulate at synapses. In fixed neurons, 18.7 ± 3.1% of synapsin-labeled terminals overlapped with DCV-pHluorin puncta (n = 616 synapses measured in four cells). Similar results were obtained for the endogenous cargo Secretogranin II (19.9 ± 3.7%, n = 493 synapses in five cells). Hence, in hippocampal neurons most synapses do not contain DCVs.

As DCVs are smaller than our resolution limit, individual DCV puncta may contain multiple DCVs. To assess this, we compared fluorescence intensity of individual puncta

upon NH_4^+ application at synapses and extrasynaptic regions. DCV-pHluorin puncta showed a similar intensity distribution at synapses as outside synapses with a major population at 6 a.u. (synaptic: median 6.0, mean 7.4 ± 0.8, n = 589 puncta; extrasynaptic: median 5.7, mean 7.0 ± 0.8, n = 612 puncta; n = 8 cells; $P > 0.05$; Fig. 2, C and D). Thus, the majority of single puncta are indeed single DCVs (compare Fig. 1 D with Fig. 2, C and D), whereas some puncta comprise multiple DCVs (between one and four with 6 a.u. representing a single DCV; Fig. 1 D). These DCV clusters are present at extrasynaptic as well as synaptic sites with no specific enrichment in synapses. Electron micrographs corroborated these findings and revealed both single DCVs and DCV clusters outside synaptic areas (Fig. S2 D). On average 1.4 DCVs were present per synapse section (mean DCV diameter: 68.9 ± 1.0 nm; Fig. 2, E and F), and almost half of the sections did not contain DCVs (Fig. 2 G). In sections with DCVs, most DCVs were randomly distributed in the terminal, whereas ±22% were physically attached (docked) to the active zone (Fig. 2 G, inset). Together, these data show that most synapsin-labeled terminals do not contain DCVs and that DCV clusters are not enriched in terminals at rest.

Yet, the majority of DCV release events occurred at synapsin-positive regions (synaptic: 66%, 315 events; extrasynaptic: 34%, 165 events; n = 34 cells; n = 3; Fig. 2 H), and DCV release rates were much slower at extrasynaptic sites than at synapses (synaptic: 12.6 ± 0.3 vesicles/s; extrasynaptic: 7.8 ± 0.2 vesicles/s; $P < 0.05$; Fig. 2 I). In line with this observation, synaptic DCV release required less intense stimulation compared with extrasynaptic release: already after the first 50 APs, DCVs were released at synapses, whereas extrasynaptic release started only after three bursts of 50 APs (Fig. 2, I and J). Apart from the kinetic difference, no differences were observed in the size and shape of the individual release events (Fig. 2 K). Hence, DCV release probability at synapses is higher than outside these regions.

Deletion of Munc13-1 reduces and delays synaptic DCV release

To gain insight into the molecular priming mechanisms of neuronal DCV release, we tested the role of the SV priming proteins of the Munc13 family in the *munc13-1/2*–null mutant (Munc13 double knockout [KO; M13DKO]) mice. In M13DKO neurons, the number of DCVs per cell was not changed (Fig. S2 A), but DCV release was reduced by >60% compared with wild type (WT: 11.8 ± 2.3, n = 41 cells; M13DKO: 4.7 ± 1.0, n = 23 cells; $P < 0.01$; Fig. 3 A). In addition, DCV release rates were slower (WT: 0.73 ± 0.12 vesicles/s; M13DKO: 0.32 ± 0.1 vesicles/s; $P < 0.05$; Fig. 3 B), and release required more prolonged stimulation as M13DKO neurons released DCVs only after the third burst of 50 APs (Fig. 3, B and C). Hence, deletion of Munc13-1/2 strongly reduces the number and rate of DCV release events. In contrast to SV release, however, it does not totally abolish DCV release. Munc13-1 single null mutant neurons showed a similar strong reduction of DCV release, indicating that Munc13-1 is the dominant isoform supporting DCV release (Fig. S3).

Munc13-1 is highly enriched in presynaptic terminals (Kalla et al., 2006) and could thus influence the localization of DCV release. We first excluded that deletion of Munc13-1 affected DCV localization in the synapse using electron microscopy (Fig. S3, C and D). Next, using synapsin-mCherry as a synaptic marker, we found that Munc13-1/2 deletion did not change the localization of DCVs before release (Fig. S2 C and Fig. 3 D) but strongly affected the ratio of synaptic versus extrasynaptic release (Fig. 3 E) by reducing the number of synaptic release events (Fig. 3 F). This suggests that Munc13-1 specifically promotes synaptic DCV release. Consistent with this observation, Munc13-1/2 deletion affected synaptic DCV release rates much more than extrasynaptic release (WT synaptic: 0.49 ± 0.09 vesicles/s; M13DKO synaptic: 0.17 ± 0.1 vesicles/s; $P < 0.05$; WT extrasynaptic: 0.24 ± 0.08 vesicles/s; M13DKO extrasynaptic 0.16 ± 0.13 vesicles/s; Fig. 3, G and H). Hence, Munc13 deletion does not alter DCV localization or mobility at steady state. It does, however, specifically affect the amount and rate of synaptic DCV release.

M13OE increases the number of extrasynaptic DCV release events

M13OE in bovine chromaffin cells enhances DCV release (Ashery et al., 2000). To test whether similar principles apply for DCV release in neurons, we tested the effect of M13OE in WT hippocampal neurons. M13OE resulted in a more than fourfold increase in protein levels compared with endogenous levels (Fig. 4 A). Endogenous Munc13-1 showed a clear punctate localization, which overlapped with synapsin-mCherry. In contrast, overexpressed Munc13-1 was not restricted to synapses but distributed homogenously throughout the neurites (Fig. 4 B). Similar ectopic expression of Munc13-1 has been observed before (Deng et al., 2011).

M13OE did not change the total number or localization of DCVs (Fig. S2, B and C; and Fig. 4 C) but significantly increased DCV release events compared with WT (WT: 10.1 ± 1.8, n = 36; M13OE: 18.4 ± 3.2, n = 32; $P < 0.05$; Fig. 4 D). Release started earlier in M13OE neurons (Fig. 4, E and F), although this effect was rather subtle when measured regardless of the spatial localization of the events. However, as in M13DKO neurons, the preference for DCV release at synaptic sites was lost in M13OE neurons (Fig. 4 G). In contrast to Munc13 deletion, this was now caused by a specific increase in DCV release events at extrasynaptic sites (Fig. 4 H) with significantly increased vesicle release rates at these sites (WT extrasynaptic: 0.24 ± 0.04 vesicles/s; M13OE extrasynaptic: 0.36 ± 0.01 vesicles/s; $P < 0.05$; Fig. 4 I). In M13OE neurons, extrasynaptic release events occurred already during the first four stimuli. During this time window, WT neurons did not show release (Fig. 4 J). Munc13 overexpression hardly, if at all, affected synaptic release events (Fig. 4, K and L). Together, this shows that overexpression of Munc13-1 is sufficient to produce efficient DCV release at extrasynaptic sites.

A model for DCV release in neurons

The present study characterized mechanisms that control synaptic DCV release in hippocampal neurons. We found that

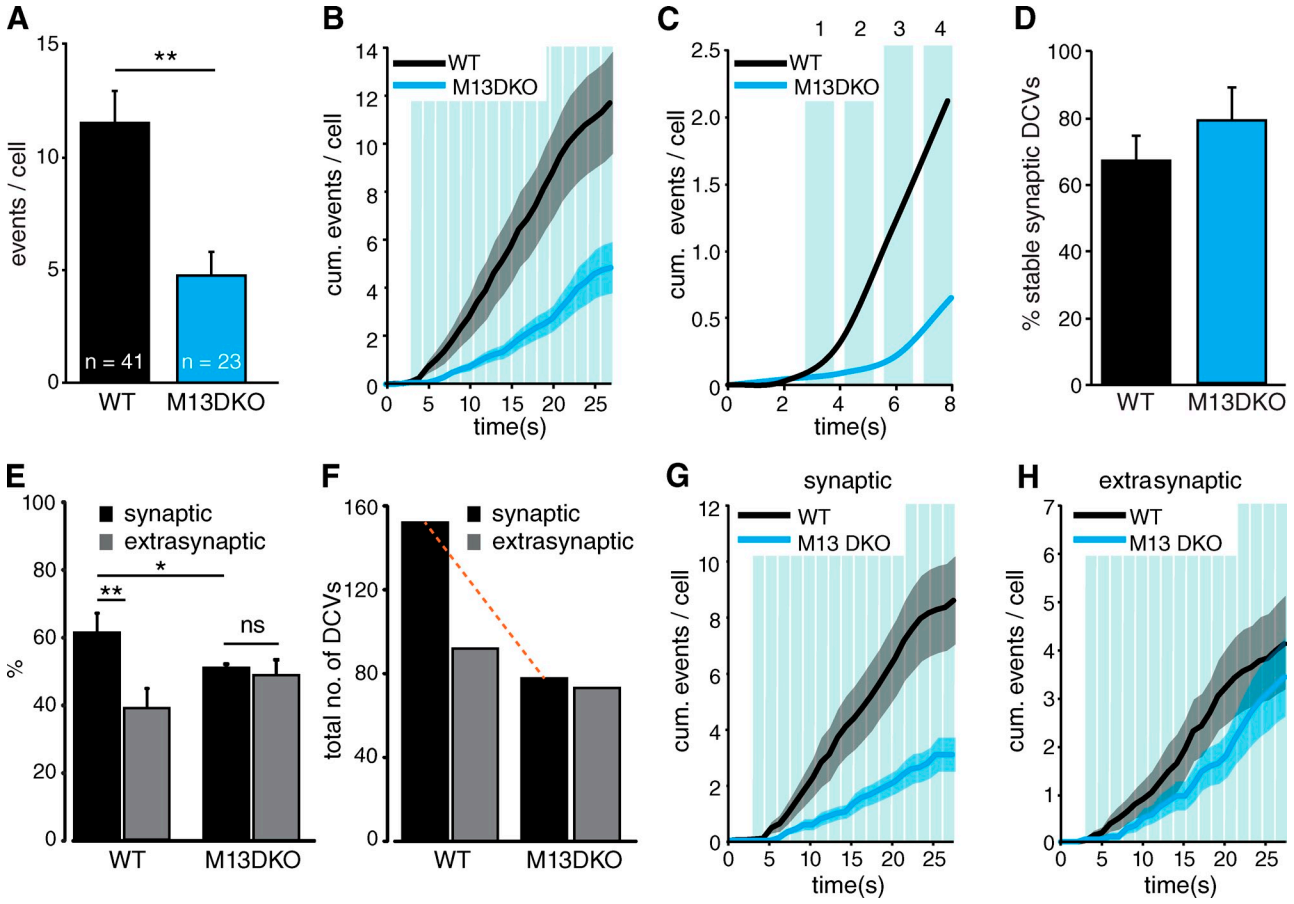

Figure 3. **Munc13 specifically reduces DCV release at synapses.** (A) Mean number of DCV release events per cell for WT and Munc13-1/2 DKO (M13DKO) neurons measured with Semaphorin-3a–pHluorin (WT: 482 events, n = 41 cells; M13DKO: 108 events, n = 23 cells; n = 4; **, $P < 0.01$). (B) Cumulative number of release events per cell. (C) Cumulative (cum.) number of release events during the first four bursts of 50 APs at 50 Hz. (D) Percentage of synaptically localized DCVs that remain synaptic during 10-s acquisition (WT: 221 vesicles, n = 6 cells; M13DKO: 146 vesicles, n = 5 cells; n = 2). (E) Percentage of synaptic and extrasynaptic DCV release events in WT and M13DKO neurons (WT: 21 cells; M13DKO: 23 cells; n = 4; *, $P < 0.05$; **, $P < 0.01$). (F) Total numbers of synaptic and extrasynaptic events show a specific loss of synaptic events (total events: WT, 255; M13DKO, 151). Red dotted line shows difference in bar heights. (G) Cumulative number of synaptic DCV release events. (H) Cumulative number of extrasynaptic DCV release events. Shading represents SEM. Data are plotted as means with SEM.

although DCVs are not enriched in synaptic terminals, they preferentially fuse at synapses. Release at extrasynaptic sites only occurs upon more prolonged stimulation compared with synaptic DCV release. We provide evidence that the synaptic priming proteins Munc13-1 and Munc13-2 are, unlike in SV secretion (Varoqueaux et al., 2002), not essential for DCV release but primarily control the localization and efficiency of DCV release: In their absence, synaptic preference of DCV fusion is lost, and remaining release events require stimulation intensities similar to extrasynaptic release events in WT neurons, whereas overexpression promotes extrasynaptic release events that do not require prolonged stimulation.

Colocalization with synapsin-mCherry and post hoc confirmation using immune detection indicated that only a small proportion (±20%) of the 100–150 DCV (clusters) present in WT, M13DKO, and M13OE neurons localizes to synaptic sites. Random sections of presynaptic profiles contained on average 1.4 DCVs with few postsynaptic DCVs, and almost half of the profiles were devoid of DCVs. Hence, our data suggest that there is no strong accumulation of DCVs in hippocampal synapses. Based on the observed DCV distribution, we expected ±20% of the DCV release events to occur at synaptic sites. Yet, we found that >65% of all events did. Release at synapses started earlier upon stimulation and reached higher release rates than extrasynaptic release. As we did not find evidence for synaptic accumulation of DCVs before release, we conclude that DCV release probability at synaptic terminals is higher than at extrasynaptic sites. As most DCVs in mammalian neurons are mobile (Silverman et al., 2005; Ramamoorthy et al., 2011), on average, only one in five synapses harbors stationary DCVs (Fig. 2; de Wit et al., 2006; Matsuda et al., 2009), which are often not predocked (Verhage et al., 1991; Silverman et al., 2005; de Wit et al., 2006, 2009b; Matsuda et al., 2009), these findings suggest that DCVs are recruited to synapses during activity and, consequently, dock and fuse from an undocked, mobile state during stimulation.

We found that loss of Munc13-1/2 strongly reduced DCV release and that Munc13-1 is the dominant isoform supporting DCV release. Hence, Munc13 emerges as a general priming factor for regulated secretion of different types of secretory vesicles (SVs and DCVs). However, almost 40% of the fusion events remained in M13DKO neurons, whereas SV

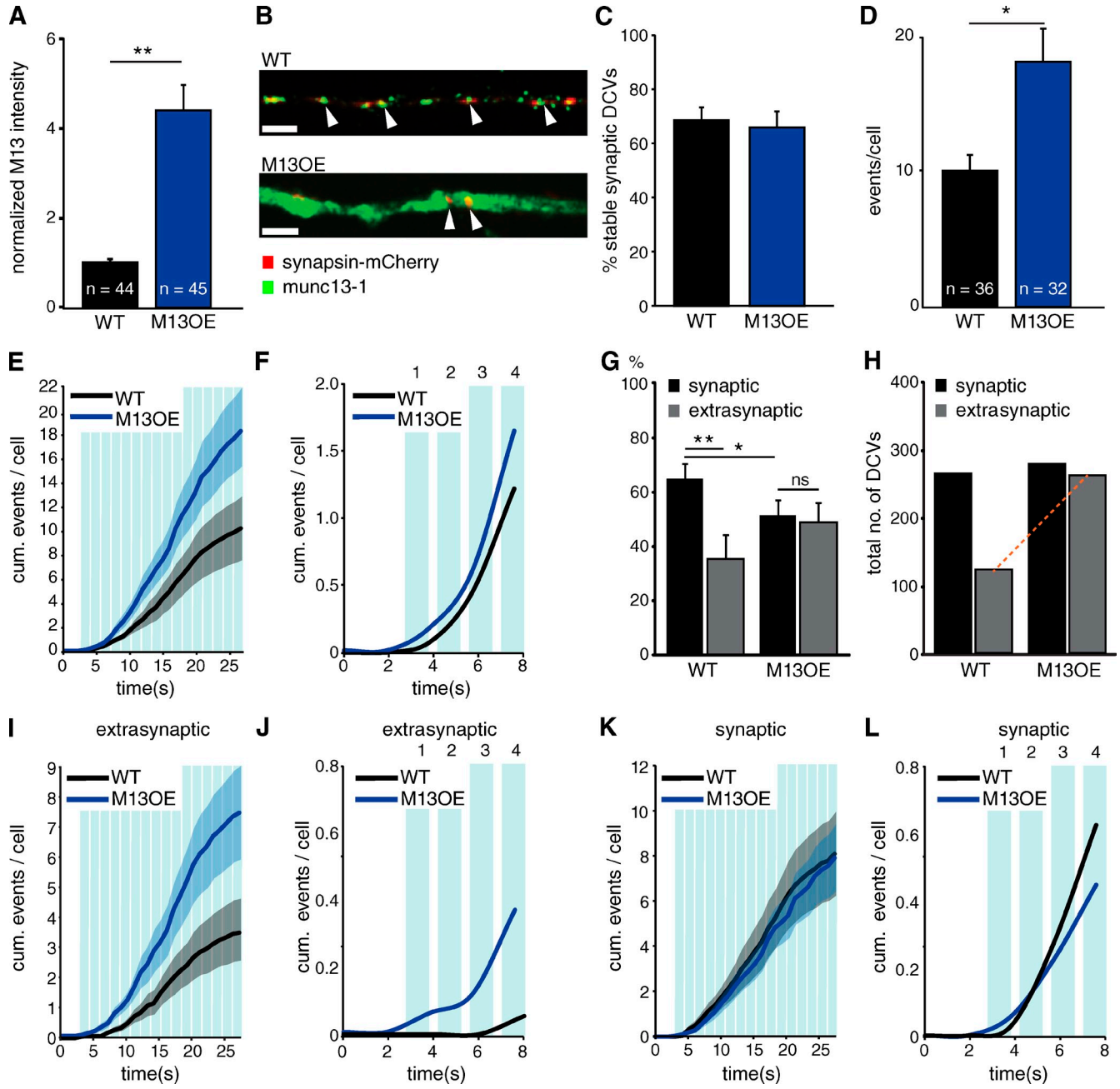

Figure 4. **M13OE increases DCV release at extrasynaptic sites.** (A) Normalized Munc13-1 intensity in WT neurons compared with neurons overexpressing Munc13-1 (M13OE, $n = 3$; **, $P < 0.001$). (B) Confocal image of a WT neuron with endogenous Munc13-1 and a WT neuron overexpressing Munc13-1 (arrowheads show synaptic localization of Munc13). Bars, 2 µm. (C) Percentage of synaptically localized DCVs that stay synaptic for 10 s (WT: 199 vesicles, $n = 7$ cells; M13OE: 170 vesicles, $n = 7$ cells). (D) Mean number of DCV release events per cell (WT: 361 events in 36 cells; M13OE: 588 events in 32 cells; $n = 3$; *, $P < 0.05$). (E) Cumulative (cum.) DCV release events per cell. (F) Cumulative number of release events during the first four bursts of 50 APs at 50 Hz. (G) Percentage of synaptic and extrasynaptic DCV release events (**, $P < 0.01$; *, $P < 0.05$). (H) Total numbers of synaptic and extrasynaptic DCV release events. Loss of synaptic preference is caused by an increase of extrasynaptic release events in M13OE. Red dotted line shows difference in bar heights. (I) Cumulative extrasynaptic DCV release events. (J) Cumulative number of events during the first four bursts at extrasynaptic sites. (K) Cumulative synaptic DCV release events. (L) Cumulative number of events during the first four bursts at synapses. Shading represents SEM. Data are plotted as means with SEM.

fusion is abolished completely in such neurons (Varoqueaux et al., 2002). In fact, our data show that impaired release efficiency is the main effect of Munc13-1/2 loss: in their absence, the first fusion events occur only after three to four episodes of 50 APs at 50 Hz. This is the same type of drastic stimulation, which may be very rare in vivo, required to trigger extrasynaptic DCV fusion in WT neurons. So, DCV fusion appears to lose its synaptic advantage upon Munc13 loss. This is consistent with the highly localized distribution of Munc13-1/2 to active zones (Kalla et al., 2006).

Conversely, M13OE leads to many more DCV fusion events at extrasynaptic sites, which also required less intense

stimulation. Upon overexpression, nonsynaptic DCV fusion events appeared to gain synaptic-like properties, and overexpression of Munc13-1 appears to be sufficient to specify extrasynaptic DCV release sites. Munc13 interacts with the t-SNARE protein syntaxin and the Sec1/Munc18 protein Munc18 (Richmond et al., 2001; Ma et al., 2011). These proteins serve as essential and minimal components for membrane fusion in many systems (Verhage et al., 2000; Rizo and Südhof, 2002; Toonen and Verhage, 2007) and are not exclusively present at synapses (Galli et al., 1995). Munc13 could organize/activate extrasynaptic t-SNARE–Munc18 complexes to increase DCV release probability at these sites.

Materials and methods

Plasmids

Semaphorin-3a–pHluorin was generated by replacing EGFP in Semaphorin-3a–EGFP (De Wit et al., 2005) with the superecliptic pHluorin (SpH) coding sequence (de Wit et al., 2009b). NPY-SpH was generated by replacing Venus (Nagai et al., 2002) with SpH (de Wit et al., 2009b). Synapsin-mCherry was a gift from A. Jeromin (Allen Brain Institute, Seattle, WA).

Laboratory animals

M13DKO mice have been described before (Varoqueaux et al., 2002). Munc13-1 KO mice were generated by replacing four exons, representing bp 2,587–2,964 of rat Munc13-1 with a neomycin resistance gene (Augustin et al., 1999). To generate Munc13-2 KO mice, a 6-kb genomic fragment containing multiple exons of the Munc13-2 gene that are shared by the two Munc13-2 splice variants (bp 2,907–3,904 of brain-specific Munc13-2 cDNA [available under GenBank accession no. U24071]; bp 1,439–2,436 of ubiquitous Munc13-2 cDNA [GenBank accession no. AF159706]) was replaced by a neomycin resistance cassette. Embryonic day 18 embryos were obtained by caesarean section of pregnant females from timed matings of Munc13-2 homozygous and Munc13-1 heterozygous mice. M13DKO embryos are stillborn, and M13DKO neurons in culture (day in vitro [DIV] 14) show neither evoked nor spontaneous release events yet form normal numbers of synapses with typical ultrastructural features. Animals were housed and bred according to institutional, Dutch, and U.S. governmental guidelines.

Primary neuronal cell culture and transfection

Dissociated hippocampal neurons were prepared from embryonic day 18 mice as previously described (de Wit et al., 2009b). Hippocampi were dissected in HBSS (Sigma-Aldrich) and digested with 0.25% trypsin (Invitrogen) for 20 min at 37°C. Hippocampi were washed and triturated with fire-polished Pasteur pipettes, counted, and plated in Neurobasal medium (Invitrogen) supplemented with 2% B-27 (Invitrogen), 1.8% Hepes, 1% GlutaMAX (Invitrogen), and 1% penicillin-streptomycin (Invitrogen). High-density cultures (25,000 neurons/well) were plated on pregrown cultures of rat glia cells (37,500 cells/well) on 18-mm glass coverslips in 12-well plates. At DIV10, neuronal cultures were transfected with calcium phosphate with DCV-pHluorin together with synapsin-mCherry (to identify synapses) and ECFP (as a neuronal morphology marker). Neurons were imaged at DIV14–DIV15.

Imaging

Coverslips were placed in an imaging chamber and perfused with Tyrode's solution (2 mM $CaCl_2$, 2.5 mM KCl, 119 mM NaCl, 2 mM $MgCl_2$, 20 mM glucose, and 25 mM Hepes, pH 7.4) and imaged on a microscope (Axio Observer.Z1; Carl Zeiss) equipped with a camera (CoolSNAP HQ; Photometrics) and an illumination unit (Polychrome IV; TILL Photonics). Images were acquired at 2 Hz with MetaMorph 6.2 software (Universal Imaging) using a 40× objective, NA 1.3. Intracellular pH was neutralized with normal Tyrode's solution containing 50 mM NH_4Cl, which replaced NaCl on an equimolar basis in the solution. A barrel pipette was used to apply NH_4^+ solution to the cells. Electrical field stimulation by parallel platinum electrodes was applied by a Master-8 system (A.M.P.I.) and a stimulus generator (A385RC; World Precision Instruments) delivering 30-mA, 1-ms pulses. The stimulus used was 16 trains of 50 APs at 50 Hz with 0.5-s interval. All imaging experiments were performed at RT (21–24°C) in the presence of 50 µM (2R)-amino-5-phosphonovaleric acid (Tocris Bioscience) and 10 µM 6,7-dinitroquinoxaline-2,3-dione (Tocris Bioscience) to block glutamatergic transmission. The imaging protocol consisted of a 30-s time lapse, applying NH_4^+ Tyrode's solution after 10 s for 10 s. Then, a 5-min recovery period was performed, in which spontaneous release was assessed during the last 60 s of this period. After this, a 100-s time lapse with electrical field stimulation was recorded. Field stimulation started after 3 s and lasted 24 s. Spontaneous events after the stimulation were counted during the last 70 s. Furthermore, ECFP and synapsin-mCherry images were acquired before and after the recording for further analysis. Neurons in which ECFP or synapsin-mCherry masks before and after stimulation shifted >1 pixel (0.165 µm) were discarded from the analysis.

Image analysis

Stacks from time-lapse recordings acquired with 0.5-s intervals were used to analyze DCV release. A 4 × 4–pixel region (0.6 × 0.6 µm) of interest was centered on each event, and the mean intensity of the fluorescence was measured with MetaMorph software. Fluorescent traces were expressed as the fluorescence change (ΔF) compared with the initial fluorescence (F_0), obtained by averaging the first four frames of the time-lapse video. Onset of exocytosis was defined as the first frame with an increase of fluorescence of two SDs above F_0. DCV release rates were measured from linear fits of the cumulative plots. Colocalization with synapsin was measured by overlaying both images in MetaMorph. A cargo-pHluorin release event or punctum was scored as synaptic when the fluorescence center of such a release event/punctum was within 200 nm (±1 pixel, the approximate minimal point spread function of our system) of the synapsin-mCherry fluorescence centroid. Extrasynaptic events were all events that did not meet this criterion. We only measured release events from neurites and excluded somatic release events. Somatic release events cannot be reliably measured using wide-field fluorescence microcopy because of the bright fluorescence from vesicles in/near the Golgi apparatus in which the intraluminal pH is not yet acidic. The total number of vesicles was automatically analyzed from the NH_4^+ application time lapse using SynD software (Schmitz et al., 2011). In Fig. 3 D and Fig. 4 C, the localization and dynamics of DCVs were determined by analyzing cargo-pHluorin–labeled vesicles during NH_4^+ application. Per neuron, four 50-µm regions containing synapses were selected for line scan measurements. DCV fluorescence peaks one SD above mean were scored for overlap with synapsin-mCherry fluorescence peaks at the first frame of a 10-s time window. During these 10 s, even the slowest moving DCVs in our system (0.29 µm/s; de Wit et al., 2006) would have traveled ±3 µm (or >18 pixels). Stable DCVs are therefore defined as DCVs that do not leave the synaptic area in 10 s.

Immunocytochemistry

After imaging, cells were fixed in 4% formaldehyde (Electron Microscopy Sciences) in PBS, pH 7.4, for 20 min at RT. Cells were washed in PBS and first permeabilized for 5 min in PBS containing 0.5% Triton X-100 (Sigma-Aldrich) and then incubated for 30 min with PBS (Gibco) containing 2% normal goat serum and 0.1% Triton X-100. Incubations with primary and secondary antibodies were performed for 1 h at RT. Primary antibodies used were polyclonal MAP2 (Abcam), monoclonal VAMP2 (Synaptic Systems), polyclonal Munc13 (Synaptic Systems), polyclonal chromogranin A, and polyclonal secretogranin II (gifts from P. Rosa, Institute of Neuroscience, Milan, Italy). Alexa Fluor–conjugated secondary antibodies were obtained from Invitrogen. Coverslips were mounted in Mowiol and examined on a confocal laser-scanning microscope (LSM 510; Carl Zeiss) with a 40× objective, NA 1.3.

Electron microscopy

Neurons were fixed at DIV14–16 for 1–2 h at RT with 0.1 M cacodylate buffer/0.25 mM $CaCl_2$/0.5 mM $MgCl_2$, pH 7.4, and processed as previously described (Wierda et al., 2007; Meijer et al., 2012). In brief, cells were postfixed for 2 h at RT with 1% osmium tetroxide/1% potassium ferro-cyanide, washed, and stained with 1% uranyl acetate for 40 min in the dark. After dehydration, cells were embedded in Epon. Cells of interest were selected using the light microscope and mounted on prepolymerized Epon blocks for thin sectioning. Ultrathin sections (~90 nm) were cut parallel to the cell monolayer, collected on single-slot, Formvar-coated copper grids, and stained in uranyl acetate and lead citrate. Synapses with a recognizable pre- and postsynaptic density were randomly selected using an electron microscope (1010; JEOL) and imaged at 100.000× using analysis software (Soft Imaging System). The observer was blinded for the

genotype. DCV distribution was measured with ImageJ (National Institutes of Health). Docked DCVs were 0 nm from the vesicle membrane to the plasma membrane.

Statistics

Throughout the paper, Student's *t* tests for unpaired data were used unless otherwise specified. If F tests showed significantly different SDs, Student's *t* tests were Welch corrected. Mann–Whitney tests were used to compare groups when one or both did not pass the normality test. To test more than two groups, Kruskal–Wallis one-way analysis of variance with post hoc Dunn's multiple comparisons test was used. Kolmogorov–Smirnov test was used to test whether distributions were normally distributed and for testing frequency distributions. Data are plotted as means with SEM.

Online supplemental material

Fig. S1 shows DCV release events in WT neurons measured with NPY-pHluorin, calcium influx upon 16 × 50 APs at 50-Hz stimulation paradigm, comparison of the effectiveness of different stimulation paradigms for DCV release, colocalization of synapsin-mCherry with endogenous VAMP2, and the number of synapses per neurite length in our culture system. Fig. S2 shows the total number of DCVs present in all genotypes with their distribution. Fig. S3 shows DCV release and EM localization in *munc13-1*–null mutant neurons. Online supplemental material is available at http://www.jcb.org/cgi/content/full/jcb.201208024/DC1.

We thank Prof. Nils Brose for Munc13-1/2 mice, Jurjen Broeke for technical assistance, Robbert Zalm for viral particles, Desiree Schut for neuronal cultures, and Rien Dekker for electron microscopy.

This work is supported by the European Union (EUSynapse 019055, EUROSPIN HEALTH-F2-2009-241498, and Synaptic Systems HEALTH-F2-2009-242167 to M. Verhage and Marie Curie MEST-CT-2005-020919 to S.K. Schmitz), National Institutes of Health (R01 DA016782-05 to A. de Jong), and the Netherlands Organization for Scientific Research (VENI 916-66-101 and TOP 91208017 to R.F. Toonen; VENI 916-36-043 to H. de Wit; Pionier/VICI 900-01-001, 834-09-002, and TOP 903-42-095 to M. Verhage; and Toptalent 021.001.076 to S.K. Schmitz).

Submitted: 14 August 2012
Accepted: 8 November 2012

References

Ashery, U., F. Varoqueaux, T. Voets, A. Betz, P. Thakur, H. Koch, E. Neher, N. Brose, and J. Rettig. 2000. Munc13-1 acts as a priming factor for large dense-core vesicles in bovine chromaffin cells. *EMBO J.* 19:3586–3596. http://dx.doi.org/10.1093/emboj/19.14.3586

Augustin, I., C. Rosenmund, T.C. Südhof, and N. Brose. 1999. Munc13-1 is essential for fusion competence of glutamatergic synaptic vesicles. *Nature*. 400:457–461. http://dx.doi.org/10.1038/22768

Bartfai, T., K. Iverfeldt, G. Fisone, and P. Serfözö. 1988. Regulation of the release of coexisting neurotransmitters. *Annu. Rev. Pharmacol. Toxicol.* 28:285–310. http://dx.doi.org/10.1146/annurev.pa.28.040188.001441

Basu, J., A. Betz, N. Brose, and C. Rosenmund. 2007. Munc13-1 C1 domain activation lowers the energy barrier for synaptic vesicle fusion. *J. Neurosci.* 27:1200–1210. http://dx.doi.org/10.1523/JNEUROSCI.4908-06.2007

Deng, L., P.S. Kaeser, W. Xu, and T.C. Südhof. 2011. RIM proteins activate vesicle priming by reversing autoinhibitory homodimerization of Munc13. *Neuron*. 69:317–331. http://dx.doi.org/10.1016/j.neuron.2011.01.005

de Wit, H., A.M. Walter, I. Milosevic, A. Gulyás-Kovács, D. Riedel, J.B. Sørensen, and M. Verhage. 2009a. Synaptotagmin-1 docks secretory vesicles to syntaxin-1/SNAP-25 acceptor complexes. *Cell*. 138:935–946. http://dx.doi.org/10.1016/j.cell.2009.07.027

De Wit, J., F. De Winter, J. Klooster, and J. Verhaagen. 2005. Semaphorin 3A displays a punctate distribution on the surface of neuronal cells and interacts with proteoglycans in the extracellular matrix. *Mol. Cell. Neurosci.* 29:40–55. http://dx.doi.org/10.1016/j.mcn.2004.12.009

de Wit, J., R.F. Toonen, J. Verhaagen, and M. Verhage. 2006. Vesicular trafficking of semaphorin 3A is activity-dependent and differs between axons and dendrites. *Traffic*. 7:1060–1077. http://dx.doi.org/10.1111/j.1600-0854.2006.00442.x

de Wit, J., R.F. Toonen, and M. Verhage. 2009b. Matrix-dependent local retention of secretory vesicle cargo in cortical neurons. *J. Neurosci.* 29:23–37. http://dx.doi.org/10.1523/JNEUROSCI.3931-08.2009

Galli, T., E.P. Garcia, O. Mundigl, T.J. Chilcote, and P. De Camilli. 1995. v- and t-SNAREs in neuronal exocytosis: a need for additional components to define sites of release. *Neuropharmacology*. 34:1351–1360. http://dx.doi.org/10.1016/0028-3908(95)00113-K

Garner, C.C., S. Kindler, and E.D. Gundelfinger. 2000. Molecular determinants of presynaptic active zones. *Curr. Opin. Neurobiol.* 10:321–327. http://dx.doi.org/10.1016/S0959-4388(00)00093-3

Gitler, D., Y. Xu, H.T. Kao, D. Lin, S. Lim, J. Feng, P. Greengard, and G.J. Augustine. 2004. Molecular determinants of synapsin targeting to presynaptic terminals. *J. Neurosci.* 24:3711–3720. http://dx.doi.org/10.1523/JNEUROSCI.5225-03.2004

Hartmann, M., R. Heumann, and V. Lessmann. 2001. Synaptic secretion of BDNF after high-frequency stimulation of glutamatergic synapses. *EMBO J.* 20:5887–5897. http://dx.doi.org/10.1093/emboj/20.21.5887

Hirokawa, N., Y. Noda, Y. Tanaka, and S. Niwa. 2009. Kinesin superfamily motor proteins and intracellular transport. *Nat. Rev. Mol. Cell Biol.* 10:682–696. http://dx.doi.org/10.1038/nrm2774

Huang, E.J., and L.F. Reichardt. 2001. Neurotrophins: roles in neuronal development and function. *Annu. Rev. Neurosci.* 24:677–736. http://dx.doi.org/10.1146/annurev.neuro.24.1.677

Jahn, R., and R.H. Scheller. 2006. SNAREs—engines for membrane fusion. *Nat. Rev. Mol. Cell Biol.* 7:631–643. http://dx.doi.org/10.1038/nrm2002

Kalla, S., M. Stern, J. Basu, F. Varoqueaux, K. Reim, C. Rosenmund, N.E. Ziv, and N. Brose. 2006. Molecular dynamics of a presynaptic active zone protein studied in Munc13-1-enhanced yellow fluorescent protein knock-in mutant mice. *J. Neurosci.* 26:13054–13066. http://dx.doi.org/10.1523/JNEUROSCI.4330-06.2006

Kim, T., M.C. Gondré-Lewis, I. Arnaoutova, and Y.P. Loh. 2006. Dense-core secretory granule biogenesis. *Physiology (Bethesda)*. 21:124–133. http://dx.doi.org/10.1152/physiol.00043.2005

Knobloch, H.S., A. Charlet, L.C. Hoffmann, M. Eliava, S. Khrulev, A.H. Cetin, P. Osten, M.K. Schwarz, P.H. Seeburg, R. Stoop, and V. Grinevich. 2012. Evoked axonal oxytocin release in the central amygdala attenuates fear response. *Neuron*. 73:553–566. http://dx.doi.org/10.1016/j.neuron.2011.11.030

Ludwig, M., and G. Leng. 2006. Dendritic peptide release and peptide-dependent behaviours. *Nat. Rev. Neurosci.* 7:126–136. http://dx.doi.org/10.1038/nrn1845

Ma, C., W. Li, Y. Xu, and J. Rizo. 2011. Munc13 mediates the transition from the closed syntaxin-Munc18 complex to the SNARE complex. *Nat. Struct. Mol. Biol.* 18:542–549. http://dx.doi.org/10.1038/nsmb.2047

Matsuda, N., H. Lu, Y. Fukata, J. Noritake, H. Gao, S. Mukherjee, T. Nemoto, M. Fukata, and M.M. Poo. 2009. Differential activity-dependent secretion of brain-derived neurotrophic factor from axon and dendrite. *J. Neurosci.* 29:14185–14198. http://dx.doi.org/10.1523/JNEUROSCI.1863-09.2009

McAllister, A.K., L.C. Katz, and D.C. Lo. 1999. Neurotrophins and synaptic plasticity. *Annu. Rev. Neurosci.* 22:295–318. http://dx.doi.org/10.1146/annurev.neuro.22.1.295

Meijer, M., P. Burkhardt, H. de Wit, R.F. Toonen, D. Fasshauer, and M. Verhage. 2012. Munc18-1 mutations that strongly impair SNARE-complex binding support normal synaptic transmission. *EMBO J.* 31:2156–2168. http://dx.doi.org/10.1038/emboj.2012.72

Meyer-Lindenberg, A., G. Domes, P. Kirsch, and M. Heinrichs. 2011. Oxytocin and vasopressin in the human brain: social neuropeptides for translational medicine. *Nat. Rev. Neurosci.* 12:524–538. http://dx.doi.org/10.1038/nrn3044

Nagai, T., K. Ibata, E.S. Park, M. Kubota, K. Mikoshiba, and A. Miyawaki. 2002. A variant of yellow fluorescent protein with fast and efficient maturation for cell-biological applications. *Nat. Biotechnol.* 20:87–90. http://dx.doi.org/10.1038/nbt0102-87

Poo, M.M. 2001. Neurotrophins as synaptic modulators. *Nat. Rev. Neurosci.* 2:24–32. http://dx.doi.org/10.1038/35049004

Ramamoorthy, P., Q. Wang, and M.D. Whim. 2011. Cell type-dependent trafficking of neuropeptide Y-containing dense core granules in CNS neurons. *J. Neurosci.* 31:14783–14788. http://dx.doi.org/10.1523/JNEUROSCI.2933-11.2011

Rhee, J.S., A. Betz, S. Pyott, K. Reim, F. Varoqueaux, I. Augustin, D. Hesse, T.C. Südhof, M. Takahashi, C. Rosenmund, and N. Brose. 2002. Beta phorbol ester- and diacylglycerol-induced augmentation of transmitter release is mediated by Munc13s and not by PKCs. *Cell*. 108:121–133. http://dx.doi.org/10.1016/S0092-8674(01)00635-3

Richmond, J.E., R.M. Weimer, and E.M. Jorgensen. 2001. An open form of syntaxin bypasses the requirement for UNC-13 in vesicle priming. *Nature*. 412:338–341. http://dx.doi.org/10.1038/35085583

Rizo, J., and T.C. Südhof. 2002. Snares and Munc18 in synaptic vesicle fusion. *Nat. Rev. Neurosci.* 3:641–653.

Rosenmund, C., J. Rettig, and N. Brose. 2003. Molecular mechanisms of active zone function. *Curr. Opin. Neurobiol.* 13:509–519. http://dx.doi.org/10.1016/j.conb.2003.09.011

Samson, A.L., and R.L. Medcalf. 2006. Tissue-type plasminogen activator: a multifaceted modulator of neurotransmission and synaptic plasticity. *Neuron*. 50:673–678. http://dx.doi.org/10.1016/j.neuron.2006.04.013

Schlager, M.A., and C.C. Hoogenraad. 2009. Basic mechanisms for recognition and transport of synaptic cargos. *Mol. Brain*. 2:25. http://dx.doi.org/10.1186/1756-6606-2-25

Schmitz, S.K., J.J. Hjorth, R.M. Joemai, R. Wijntjes, S. Eijgenraam, P. de Bruijn, C. Georgiou, A.P. de Jong, A. van Ooyen, M. Verhage, et al. 2011. Automated analysis of neuronal morphology, synapse number and synaptic recruitment. *J. Neurosci. Methods*. 195:185–193. http://dx.doi.org/10.1016/j.jneumeth.2010.12.011

Shakiryanova, D., A. Tully, and E.S. Levitan. 2006. Activity-dependent synaptic capture of transiting peptidergic vesicles. *Nat. Neurosci.* 9:896–900. http://dx.doi.org/10.1038/nn1719

Silverman, M.A., S. Johnson, D. Gurkins, M. Farmer, J.E. Lochner, P. Rosa, and B.A. Scalettar. 2005. Mechanisms of transport and exocytosis of dense-core granules containing tissue plasminogen activator in developing hippocampal neurons. *J. Neurosci.* 25:3095–3106. http://dx.doi.org/10.1523/JNEUROSCI.4694-04.2005

Sørensen, J.B. 2009. Conflicting views on the membrane fusion machinery and the fusion pore. *Annu. Rev. Cell Dev. Biol.* 25:513–537. http://dx.doi.org/10.1146/annurev.cellbio.24.110707.175239

Südhof, T.C. 2004. The synaptic vesicle cycle. *Annu. Rev. Neurosci.* 27:509–547. http://dx.doi.org/10.1146/annurev.neuro.26.041002.131412

Südhof, T.C., and J.E. Rothman. 2009. Membrane fusion: grappling with SNARE and SM proteins. *Science*. 323:474–477. http://dx.doi.org/10.1126/science.1161748

Toonen, R.F., and M. Verhage. 2007. Munc18-1 in secretion: lonely Munc joins SNARE team and takes control. *Trends Neurosci.* 30:564–572. http://dx.doi.org/10.1016/j.tins.2007.08.008

Varoqueaux, F., A. Sigler, J.S. Rhee, N. Brose, C. Enk, K. Reim, and C. Rosenmund. 2002. Total arrest of spontaneous and evoked synaptic transmission but normal synaptogenesis in the absence of Munc13-mediated vesicle priming. *Proc. Natl. Acad. Sci. USA*. 99:9037–9042. http://dx.doi.org/10.1073/pnas.122623799

Verhage, M., and R.F. Toonen. 2007. Regulated exocytosis: merging ideas on fusing membranes. *Curr. Opin. Cell Biol.* 19:402–408. http://dx.doi.org/10.1016/j.ceb.2007.05.002

Verhage, M., H.T. McMahon, W.E. Ghijsen, F. Boomsma, G. Scholten, V.M. Wiegant, and D.G. Nicholls. 1991. Differential release of amino acids, neuropeptides, and catecholamines from isolated nerve terminals. *Neuron*. 6:517–524. http://dx.doi.org/10.1016/0896-6273(91)90054-4

Verhage, M., A.S. Maia, J.J. Plomp, A.B. Brussaard, J.H. Heeroma, H. Vermeer, R.F. Toonen, R.E. Hammer, T.K. van den Berg, M. Missler, et al. 2000. Synaptic assembly of the brain in the absence of neurotransmitter secretion. *Science*. 287:864–869. http://dx.doi.org/10.1126/science.287.5454.864

Wierda, K.D., R.F. Toonen, H. de Wit, A.B. Brussaard, and M. Verhage. 2007. Interdependence of PKC-dependent and PKC-independent pathways for presynaptic plasticity. *Neuron*. 54:275–290. http://dx.doi.org/10.1016/j.neuron.2007.04.001

Wong, M.Y., C. Zhou, D. Shakiryanova, T.E. Lloyd, D.L. Deitcher, and E.S. Levitan. 2012. Neuropeptide delivery to synapses by long-range vesicle circulation and sporadic capture. *Cell*. 148:1029–1038. http://dx.doi.org/10.1016/j.cell.2011.12.036

Xu, T., and P. Xu. 2008. Searching for molecular players differentially involved in neurotransmitter and neuropeptide release. *Neurochem. Res.* 33:1915–1919. http://dx.doi.org/10.1007/s11064-008-9648-2